Kinetic Study of Vibrational Energy Transfer from a Wide Range of Vibrational Levels of $O_2(X^3\Sigma_g^-, v = 6-12)$ to CF_4†

Shinji Watanabe,§ Hidekazu Fujii,‡ Hiroshi Kohguchi,§ Takayuki Hatano,‡ Ikuo Tokue,‡ and Katsuyoshi Yamasaki*,§

Department of Chemistry, Graduate School of Science, Hiroshima University, 1-3-1 Kagamiyama, Higashi-Hiroshima, Hiroshima 739-8526, Japan, and Department of Chemistry, Niigata University, Ikarashi, Niigata 950-2181, Japan

Received: March 13, 2008; Revised Manuscript Received: April 25, 2008

A wide range of vibrational levels of $O_2(X^3\Sigma_g^-, v = 6-13)$ generated in the ultraviolet photolysis of O_3 was selectively detected by the laser-induced fluorescence (LIF) technique. The time-resolved LIF-excited $B^3\Sigma_u^- - X^3\Sigma_g^-$ system in the presence of CF_4 has been recorded and analyzed by the integrated profiles method (IPM). The IPM permitted us to determine the rate coefficients $k_v^{CF_4}$ for vibrational relaxation of $O_2(X^3\Sigma_g^-, v = 6-12)$ by collisions with CF_4. Energy transfer from O_2 ($v = 6-12$) to CF_4 is surprisingly efficient compared to that of other polyatomic relaxation partners studied so far. The $k_v^{CF_4}$ increases with vibrational quantum number v from $[1.5 \pm 0.2(2\sigma)] \times 10^{-12}$ for $v = 6$ to $[7.3 \pm 1.5(2\sigma)] \times 10^{-11}$ for $v = 12$, indicating that the infrared-active ν_3 vibrational mode of CF_4 mainly governs the energy transfer with $O_2(X^3\Sigma_g^-, v = 6-12)$. The correlation between the rate coefficients and fundamental infrared intensities has been discussed based on a comparison of the efficiency of energy transfer by several collision partners.

Introduction

The time-resolved laser excited fluorescence technique has been widely used for the study of vibrational relaxation since the mid 1960s.[1–4] In general, direct photoexcitation from a vibrationless level to highly vibrationally excited levels is difficult due to small transition probabilities. In contrast, preparation and detection of the relatively low vibrational levels $v < 8$ of $O_2(X^3\Sigma_g^-)$ are difficult not only because O_2 is infrared-inactive but also because the emissive vibrational levels of the $B^3\Sigma_u^-$ state combine with only the high vibrational levels of the $X^3\Sigma_g^-$ state.

In their pioneering work, Wodtke and co-workers[5] have employed the stimulated emission pumping (SEP) technique and applied it to prepare a single highly excited vibrational level of relatively small molecules. They have measured the rate coefficients for vibrational relaxation of $O_2(X^3\Sigma_g^-, v = 15-26)$ by triatomic molecules (CO_2, N_2O, and O_3),[6] finding simple propensities that the efficiency of V−V energy transfer from $O_2(X^3\Sigma_g^-)$ is higher at stronger infrared-active vibrational modes with a smaller energy mismatch between the vibrational quanta of $O_2(X^3\Sigma_g^-)$ and the relaxation partners. The SEP is the most sophisticated technique to study the elementary processes of a single vibrational level; however, it costs three tunable laser systems for the sequence of pump−dump−probe, and high densities of parent molecules are needed for preparing the vibrational level of interest.

Park and Slanger[7] photolyzed O_3 at 248 nm and detected vibrationally excited $O_2(X^3\Sigma_g^-, v = 8-22)$ by the laser-induced fluorescence (LIF) technique. They have made a nonlinear kinetic analysis, determining the rate coefficients for vibrational energy transfer to O_2 and N_2 and reporting that the energy transfer to O_2 is mainly governed by single-quantum relaxation ($\Delta v = 1$) and that relaxation by N_2 proceeds via a double-quantum mechanism ($\Delta v = 2$). They also have shown that the nascent vibrational distributions of $O_2(X^3\Sigma_g^-)$ are higher at lower vibrational levels.

Smith and co-workers[8–10] have measured the state-specific rate coefficients for the relaxation of $O_2(v = 8-11$, 21, and 22) by collisions with He, O_2, N_2, NO_2, CO_2, N_2O, and CH_4 (relaxation by NO_2 was observed only for $v = 8-11$). They generated $O_2(X^3\Sigma_g^-, v \leq 11)$ by a reaction $O(^3P) + NO_2 \rightarrow O_2(v) + NO$[8,9] and $O_2(X^3\Sigma_g^-, v = 21$ and 22) by the photolysis of O_3 at 266 nm.[10] They have shown that the vibrational level dependence of the rate coefficients is well-reproduced by theoretical calculations by Hernández et al.[11]

We have recently found that CF_4 is a very efficient relaxation partner for $v = 8$ of $O_2(X^3\Sigma_g^-)$.[12] O_3 was photolyzed at 266 nm in the presence of CF_4, and generated $O_2(X^3\Sigma_g^-, v = 8$ and 9) was detected by LIF. The time-resolved LIF intensities of $v = 8$ and 9 were analyzed by the integrated profiles method (IPM) originally developed by the author's group.[13,14] The rate coefficient for relaxation of $O_2(X^3\Sigma_g^-, v = 8)$ by CF_4, $[1.4 \pm 0.3(2\sigma)] \times 10^{-11}$ cm^3 molecule^{-1} s^{-1}, is the largest in those reported by any other relaxation partners. The energy mismatch ΔE of the process, $O_2(v) + CF_4(v_3 = 0) \rightarrow O_2(v-1) + CF_4(v_3 = 1) + \Delta E$, is $+114$ cm^{-1} for $v = 8$ and decreases with an increase in the vibrational quantum number up to $v = 13$ with $\Delta E = +0.6$ cm^{-1}, suggesting that the efficiency of energy transfer from $O_2(X^3\Sigma_g^-, v)$ to CF_4 increases up to around $v = 13$. In the present study, we have performed systematic measurements for determining the rate coefficients for V−V energy transfer of an extended range of the vibrational levels of $O_2(v = 6-12)$ to CF_4 and found the strong vibrational level dependence.

† Part of the "Stephen R. Leone Festschrift".

* To whom correspondence should be addressed. Fax: +81-82-424-7405. E-mail: kyam@hiroshima-u.ac.jp.

§ Hiroshima University.

‡ Niigata University.

10.1021/jp802201m CCC: $40.75
Published on Web 07/01/2008

Experimental Section

The details of the experimental apparatus have been described elsewhere.[12,15,16] It has been well-known that there are main two channels in the UV photolysis of O_3

$$O_3 + h\nu \rightarrow O(^1D_2) + O_2(a^1\Delta_g) \quad (1)$$

with $\phi \approx 0.9 \pm 0.1$,[17–19] and

$$O_3 + h\nu \rightarrow O(^3P_J) + O_2(X^3\Sigma_g^-) \quad (2)$$

The vibrationally excited $O_2(X^3\Sigma_g^-)$ generated in the minor process in eq 2 is the target of the present study. A side reaction

$$O(^1D_2) + O_3 \rightarrow O_2(X^3\Sigma_g^-, v \leq 30) + O_2 \quad (3)$$

may generate high vibrational levels $v \geq 23$.[20,21] Wodtke and co-workers[22,23] have found that vibrational levels $v \geq 23$ of $O_2(X^3\Sigma_g^-)$ show multiquantum relaxation ($\Delta v \approx 9$) by collisions with O_2, although the cause of the large change in v remains as yet unresolved. It should be noted that this extraordinary relaxation was observed in a large amount of O_2 (typical pressure was 200 Torr). In the present experiments, on the other hand, the partial pressure of O_2 generated in the photolysis is less than 1 mTorr, and Ar as a buffer gas is the relatively efficient quencher; the rate coefficient for $O(^1D) + Ar \rightarrow O(^3P) + Ar$ is $(8 \pm 3) \times 10^{-13}$ cm^3 molecule^{-1} s^{-1}.[24] Therefore, reaction 3 does not disturb the present measurements.

O_3 at 298 ± 2 K was photolyzed at 266 nm with a Nd:YAG laser (Continuum YG660-20) in the present study. The highest vibrational level of $O_2(X^3\Sigma_g^-)$ generated with the excess energy at room temperature, $h\nu + (3/2)k_BT - D_0(O_2-O) = 29417$ cm^{-1}, is $v = 22$,[10,25] where k_B is Boltzmann's constant, and high vibrational levels ($v \geq 23$) are not generated in the present photolysis.

$O_2(X^3\Sigma_g^-, v = 6-13)$ was detected via LIF in the $B^3\Sigma_u^- - X^3\Sigma_g^-$ Schumann–Runge system with a Nd^{3+}:YAG laser (Spectron SL803 or Spectra Physics CGR-130)-pumped frequency-doubled dye laser (Lambda Physik LPD3002 with a SHG crystal). All of the vibrational levels of the $B^3\Sigma_u^-$ state interact with at least four repulsive states ($^1\Pi_u$, $^3\Sigma_u^+$, $^3\Pi_u$, $^5\Pi_u$) and undergo efficient predissociation.[26,27] The fluorescence quantum yields of $v' = 0$, $\phi_f(v = 0) \approx 0.05-0.1\%$, and $v' = 2$, $\phi_f \approx 0.01-0.025\%$,[27–30] are small but larger than those of any other vibrational levels (v' is the vibrational quantum number of the $B^3\Sigma_u^-$ state). The fluorescence from $v' = 0$ or 2 was excited and detected with a photomultiplier tube (Hamamatsu R1104). Several band-pass filters with 10 or 40 nm bandwidths (full width at half-maximum) were used to monitor the specific vibrational bands associated with the vibrational levels of interest. The fluences of the photolysis and probe lasers were monitored with a joule meter (GENTEC ED-100A) or PIN photodiode (Hamamatsu S1722-02).

To record the time profiles of the LIF intensities, the wavelength of the probe laser was tuned to a rotational line, after which time delays between the photolysis and probe laser were automatically scanned with a pulse delay controller made in house. The buffer gas (Ar) at 50 Torr is sufficient for rapid rotational relaxation within at most 10 ns after the photolysis in the present experiments. Therefore, LIF intensity excited via a single rotational line represents the time evolution of the population in a vibrational level of interest. The typical number of data points in a time profile was 2000, and the step size was varied (50–300 ns) according to the time scales of the profiles. Five to ten time profiles were recorded and averaged to increase the signal-to-noise ratios.

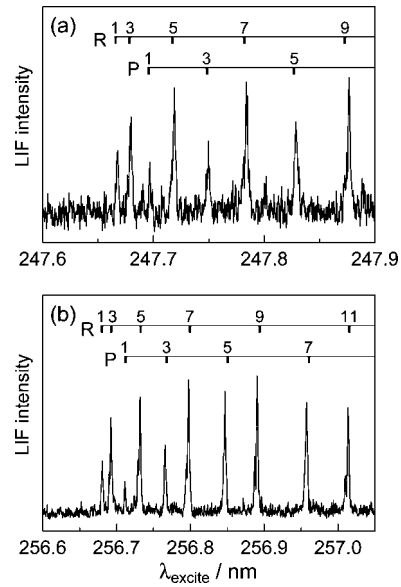

Figure 1. Rotationally resolved laser-induced fluorescence excitation spectra of the $B^3\Sigma_u^- - X^3\Sigma_g^-$ system of O_2. (a) 0–6 band and (b) 0–7 band. The rotational assignment of the P- and R- branches is made with the quantum numbers of total angular momentum without electronic spin. The delay times between the photolysis and probe laser were 10 μs for both spectra.

O_3 was prepared by an electrical discharge in high-grade O_2 (Toyo-Sanso, >99.9995%) with a synthesizer made in house and stored in a 3 dm^3 glass bulb with Ar (10% dilution). The total pressure of a sample gas was monitored with a capacitance manometer (Baratron 122A). The total pressure measurement together with the mole fractions as measured with calibrated flow controllers (Tylan FC-260KZ and STEC SEC-400 mark3) gave the partial pressures of the reagents. A typical pressure of O_3 was 9 mTorr. High-grade CF_4 (Showa-Denko, 99.99%) and Ar (Nihon-Sanso, >99.9999%) were used without further purification.

Results and Discussion

LIF Excitation Spectra of $O_2(B^3\Sigma_u^- - X^3\Sigma_g^-)$. Figure 1 shows the fluorescence excitation spectra of the 0–6 and 0–7 bands. There are six main branches and six satellite branches in a $^3\Sigma_u^- - ^3\Sigma_g^-$ system.[31] The satellite branches in the spectra, however, are too weak to observe. The three spin components of the main branches are not clearly resolved due not only to the insufficient resolution (~0.001 nm) of the probe laser but also due to fast predissociation of the excited state. Nevertheless, the assignment of the spectra to only the odd rotational quantum numbers N for the P- and R-branches has been made, indicating that the rotational levels of the O_2 in the $X^3\Sigma_g^-$ state are detected. The transition wavelengths of the $0-v$ and $2-(v+1)$ bands of the $B^3\Sigma_u^- - X^3\Sigma_g^-$ system are nearly identical because of $2\Delta G_{v'+1/2} \approx \Delta G_{v+1/2}$, and consequently, simultaneous excitation of the two bands is unavoidable. Band-pass filters enabled selective detection of the fluorescence from $v' = 0$ or 2. A band-pass filter whose maximum transmittance is at 337.0 nm was used to detect the 0–14 band (337.1 nm) and partly blocks the 2–15 band (335.8 nm). Also, the Franck–Condon factor[32] of the 0–14 band, 0.1519, is about 2 times larger than that of the 2–15 band, 0.07123, and the detection system has high detectivity for $v' = 0$. To detect the fluorescence from $v' = 2$, the 2–21 band at 437.4 nm was monitored with a band-pass filter (435.8 nm), and the large Franck–Condon factor of the 2–21 band, 0.1185,

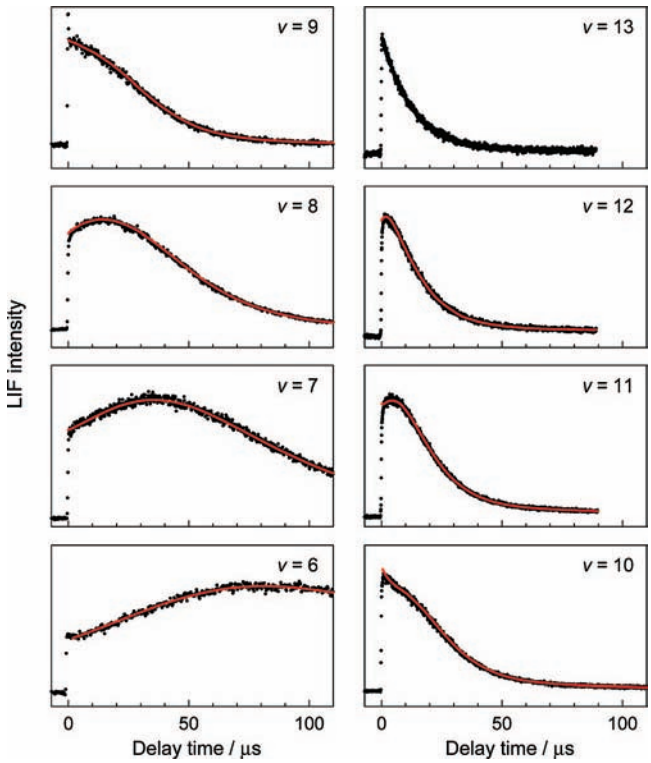

Figure 2. Time-resolved LIF intensities of $v = 6-13$ of $O_2(X^3\Sigma_g^-)$. The abscissas are the delay times between the photolysis and probe laser. All of the profiles were recorded in the presence of 100 mTorr of CF_4 in 50 Torr of Ar. The step sizes of the time scans were 265 ns for $v = 6$, 135 ns for $v = 7-9$, 75 ns for $v = 10$, and 50 ns for $v = 11-13$. The laser fluences remained constant during the measurements. The red lines in the profiles denote the time-dependent LIF intensities calculated using eq 16.

compared to 0.008476 of 0−20 (442.4 nm) offers a great advantage to selective detection of the 2−v bands. Neither of the band heads of the 2−7 and 2−8 bands, 248.07 nm and 256.96 nm, respectively overlap with P($N < 7$) and R($N < 11$) of the 0−6 band or P($N < 5$) and R($N < 9$) of the 0−7 band (Figure 1).

Vibrational Energy Transfer between $O_2(X^3\Sigma_g^-)$ and CF_4. The LIF intensities of the levels $v = 6-13$ in the presence of CF_4 at 100 mTorr as a function of the delay time between the photolysis and probe lasers are shown in Figure 2. Clearly, the higher vibrational levels decay faster than the lower vibrational levels. The time profiles of all of the levels recorded in the absence of CF_4 did not show obvious growth or decay over the identical time scale, which is consistent with the estimated first-order rate of diffusion loss of 280 s^{-1} at 50 Torr of Ar.[16] Therefore, the observed growth in all of the profiles except $v = 13$ is the effect of relaxation by the collisions of CF_4. The decay profile of the level $v = 13$ is rather single-exponential, suggesting that (i) the level $v = 14$ decays much more slowly than $v = 13$ or (ii) the populations in the levels $v > 13$ are too small to make the profile of $v = 13$ nonexponential. This is not case (i) because the time profiles of $v = 14$ recorded in the preliminary measurements also show single-exponential decay with almost identical time constant with that of $v = 13$. As for case (ii), there have unfortunately been few reports on the nascent vibrational distributions of O_2 generated in the UV photolysis of O_3 at around 250 nm. Park and Slanger[7] have measured the rate coefficients for vibrational energy transfer of $O_2(X^3\Sigma_g^-, v)$ by O_2 using 248 nm photolysis of O_3 and also determined the nascent vibrational distributions of $O_2(X^3\Sigma_g^-, v)$.

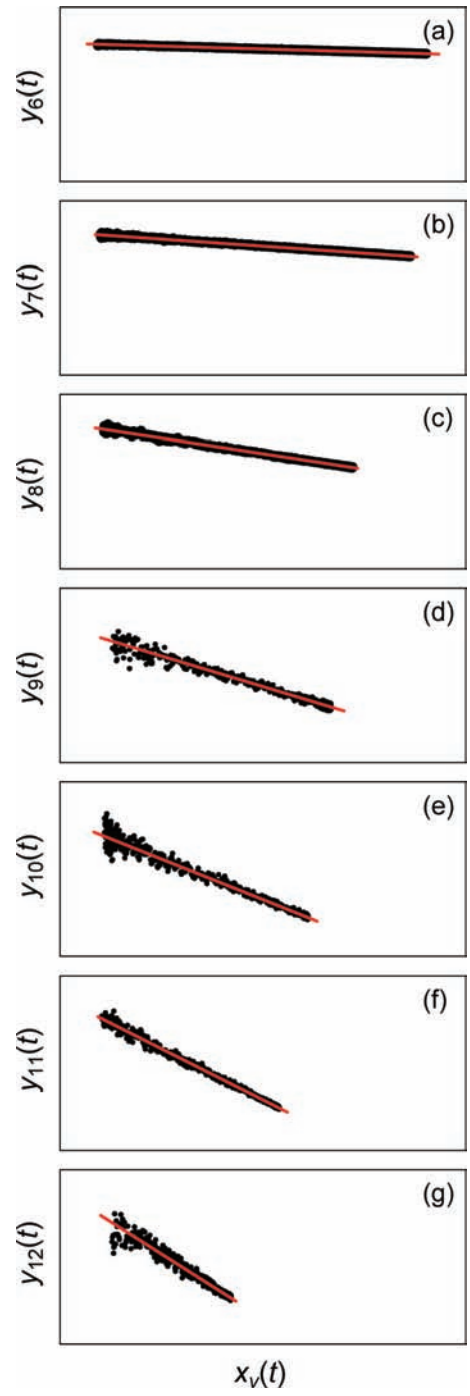

Figure 3. The IPM plots made by eq 12; $y_v(t)$ and $x_v(t)$ are defined by eqs 13 and 14, respectively: $v = 6$, (a); $v = 7$, (b); $v = 8$, (c); $v = 9$, (d); $v = 10$, (e); $v = 11$, (f); $v = 12$, (g). All of the ranges of the abscissas and ordinates of the frames are identical: 1.5 for abscissa and 2.4×10^5 s^{-1} for ordinate. Analyzed data were measured under identical conditions as those in Figure 2; the CF_4 pressure was 100 mTorr, and the total pressure was 50 Torr of Ar. The slopes given by a linear regression (red lines) correspond to the apparent pseudo-first-order decay rates of the vibrational levels.

Their results show that the populations at low levels at around $v = 8$ are dominant over those of high levels at $v \sim 14$ by an order of magnitude. Geiser et al.,[33] on the other hand, have employed REMPI coupled with the TOF of imaging technique of the $O(^3P)$ fragment in the photolysis at 266 nm, reporting vibrational distributions with two peaks at $v \sim 5$ and 9 and flat populations from $v \sim 12$ to 21 based on the measurements of the translational energies of a single spin−orbit state $O(^3P_2)$.

TABLE 1: Rate Coefficients for Vibrational Relaxation of $O_2(X^3\Sigma_g^-, v)$ by Collisions with CF_4[a]

v	$\Delta G_{v+1/2}$[b]	CO_2[c]	NO_2[c]	N_2O[c]	CH_4[c]	CF_4[d]
5						
	1441					15 ± 2
6						
	1418					59 ± 10
7						
	1395	4.7 ± 0.6	7.0 ± 0.8	16 ± 2	100 ± 20	140 ± 30
8						
	1372	2.7 ± 0.2	6.8 ± 1.0	16 ± 4	66 ± 10	320 ± 70
9						
	1350	3.2 ± 0.2	9.3 ± 1.0	24 ± 8	57 ± 20	450 ± 100
10						
	1327	2.6 ± 0.2	7.0 ± 2.0	35 ± 4		560 ± 120
11						
	1304					730 ± 150
12						

[a] Rate coefficients are in units of 10^{-13} cm^3 molecule^{-1} s^{-1}, and the confidence limits are 2σ. [b] Vibrational spacings in units of cm^{-1}. [c] Ref 9. [d] This work.

Although the nascent vibrational distributions reported by the two groups are significantly different and the cause of the discrepancy remains unclear, the time profiles observed in the present study are consistent with the distributions reported by Park and Slanger.

The kinetic scheme of $O_2(v)$ generated in the photolysis is as follows:

$$O_2(v+1) + CF_4 \xrightarrow{k_{v+1}^{CF_4}} O_2(v) + CF_4 \quad (4)$$

$$O_2(v+1) + Ar \xrightarrow{k_{v+1}^{Ar}} O_2(v) + Ar \quad (5)$$

$$O_2(v) + CF_4 \xrightarrow{k_v^{CF_4}} O_2(v-1) + CF_4 \quad (6)$$

$$O_2(v) + Ar \xrightarrow{k_v^{Ar}} O_2(v-1) + Ar \quad (7)$$

$$O_2(v) \xrightarrow{k_v^{diff}} \text{diffusion} \quad (8)$$

where k_v^M is the rate coefficient for vibrational relaxation of a level v by collisions with M and k_v^{diff} is the first-order rate coefficient for diffusion loss of a level v. Here, the assumption of single-quantum relaxation is made. The reported rate coefficients for relaxation of $O_2(X^3\Sigma_g^-, v = 11-21)$ by collisions with O_3 decrease from 5.5×10^{-12} cm^3 molecule^{-1} s^{-1} for $v = 21$ to 9×10^{-14} cm^3 molecule^{-1} s^{-1} for $v = 11$[6] and the rate coefficients for $v < 11$ are expected to be smaller than that for $v = 11$. The first-order rate coefficient of relaxation at 9 mTorr of O_3, therefore, is estimated to be less than 26 s^{-1} and negligibly small. The rate equation for the population of the vibrational level v is given to be

$$\frac{d[v]}{dt} = -\left(k_v^{CF_4}[CF_4] + k_v^{Ar}[Ar] + k_v^{diff}\right)[v] + \left(k_{v+1}^{CF_4}[CF_4] + k_{v+1}^{Ar}[Ar]\right)[v+1] \quad (9a)$$

$$\equiv -\left(k_v + k_v^{diff}\right)[v] + k_{v+1}[v+1] \quad (9b)$$

where k_v is defined by $k_v^{CF_4}[CF_4] + k_v^{Ar}[Ar]$. According to the conventional kinetic analysis, the simultaneous equations for all of the initially prepared vibrational levels, including the highest level, must be solved to obtain the analytical solutions of the time evolution of a level v. The analytical expressions as general mathematical solution can be obtained; however, it is impractical to fit the recorded profiles to the expressions. The time profile of a level v is represented by an expression composed of $v_{max} - v + 1$ exponential terms, and the identical number of time-independent parameters (constants), for example, 10 exponential terms and 10 parameters, is necessary to represent the time evolution of the level $v = 13$ in the present study because $v_{max} = 22$ (v_{max} is the highest vibrational level generated with the available energy). Twenty parameters are too many to determine with a high degree of accuracy. The IPM is suitable for analyzing the time profiles recorded in the present experiments. What needs to be known is experimentally observed time profiles of the levels $v + 1$ and v; neither the information on the initial populations nor the kinetic parameters for the vibrational levels higher than $v + 1$ are necessary to make analysis.

The IPM just puts integrals in eq 9b instead of solving eq 9b

$$[v] - [v]_0 = -\left(k_v + k_v^{diff}\right)\int_0^t [v]dt' + k_{v+1}\int_0^t [v+1]dt' \quad (10)$$

where $[v]_0$ is the nascent population of the level v. Neither absolute nor relative concentrations (populations) of different vibrational levels are readily determined by the LIF technique, and eq 10 cannot be directly applied to the recorded profiles. The observed LIF intensity of a level v at time t, $I_v(t)$, is in proportion to the

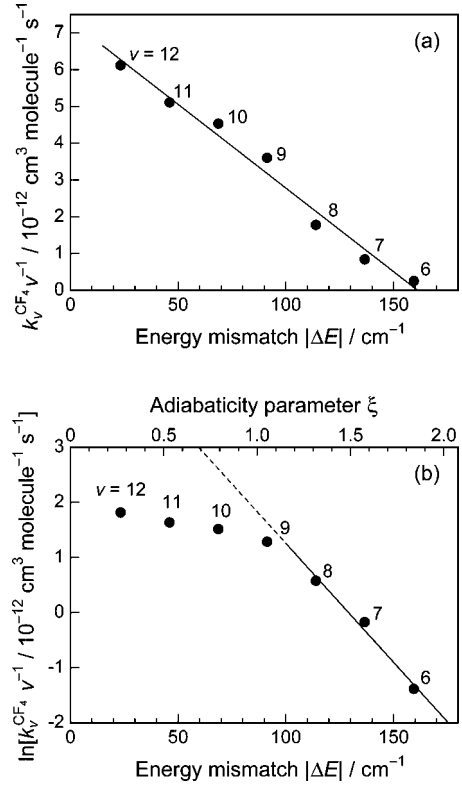

Figure 4. Energy mismatch dependence of the efficiency of relaxation of $O_2(X^3\Sigma_g^-, v = 6-12)$ by CF_4: (a) linear plot and (b) semilogarithmic plot. The line in (a) shows the result of a linear regression analysis. The top and bottom abscissa of (b) are the adiabaticity parameter and energy mismatch, respectively. The line in (b) shows the result of the semilogarithmic analysis using the data of $v = 6-8$ based on the exponential energy gap law, $k_v^{CF_4}/v = be^{-c|\Delta E|}$, with $b = 2.62 \times 10^{-10}$ cm^3 molecule^{-1} s^{-1} and $c = 0.0431$ cm.

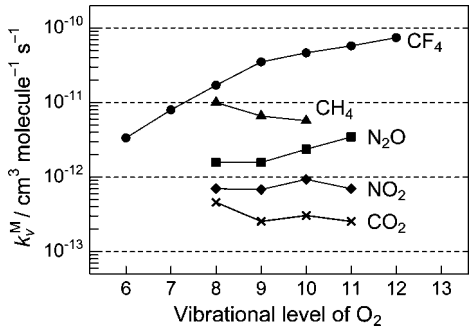

Figure 5. Vibrational level dependence of the rate coefficients for energy transfer of O_2 by collisions with several relaxation partners. The triangles for CH_4, squares for N_2O, diamonds for NO_2, and crosses for CO_2, correspond to data from ref 9. The circles represent the data of this work.

population of the vibrational level at t, $[v]$, that is, $I_v(t) = \alpha_v[v]$, where α_v is a proportionality constant (detectability), and the populations in eq 10 are replaced with observed LIF intensities.

$$I_v(t) - I_v(0) = -\left(k_v + k_v^{\mathrm{diff}}\right)\int_0^t I_v(t')\mathrm{d}t' + k_{v+1}\frac{\alpha_v}{\alpha_{v+1}}\int_0^t I_{v+1}(t')\mathrm{d}t' \quad (11)$$

Equation 11 is arranged to be

$$y_v(t) = -\left(k_v + k_v^{\mathrm{diff}}\right)x_v(t) + C_v \quad (12)$$

where

$$y_v(t) \equiv [I_v(t) - I_v(0)]/\int_0^t I_{v+1}(t')\mathrm{d}t' \quad (13)$$

$$x_v(t) \equiv \int_0^t I_v(t')\mathrm{d}t'/\int_0^t I_{v+1}(t')\mathrm{d}t' \quad (14)$$

$$C_v \equiv k_{v+1}\frac{\alpha_v}{\alpha_{v+1}} \quad (15)$$

The slope of a linear regression line in the plots $y_v(t)$ versus $x_v(t)$, called IPM plots, corresponds to $-(k_v + k_v^{\mathrm{diff}})$, giving the apparent first-order decay rate of the level v. Figure 3 shows the IPM plots made by the profiles shown in Figure 2. The linearity of all of the plots suggests that vibrational relaxation of $O_2(X^3\Sigma_g^-, v)$ by collisions with CF_4 proceeds via a single-quantum change $\Delta v = 1$, that is, $v + 1 \rightarrow v$. If some part of a level $v + 2$ is transferred to v, the IPM plots show negative curvatures.[34] However, as long as $k_{v+1\rightarrow v}[v + 1] \gg k_{v+2\rightarrow v}[v + 2]$ is satisfied, the IPM plots made of the profiles of the levels $v + 1$ and v may appear linear. As stated before, the initial populations subsequent to the photolysis have not been established yet, and the rate coefficients for multiquantum change $\Delta v > 1$ cannot be determined in the present study.

The k_v and C_v in eq 12 are determined from the IPM plots, and their reliability can be tested by the following convolution integral[34] based on the linear response theory.[35]

$$I_v(t) = I_v(0)\mathrm{e}^{-k_v t} + C_v\int_0^t I_{v+1}(x)\mathrm{e}^{-k_v(t-x)}\mathrm{d}x \quad (16)$$

Calculated $I_v(t)$, shown with the red lines in Figure 2, perfectly reproduces all of the observed time profiles. The contribution of relaxation by Ar buffer gas and diffusion loss, $k_v^{\mathrm{Ar}}[\mathrm{Ar}] + k_v^{\mathrm{diff}}$, of $v = 8$ was measured to be 7550 s^{-1} at 50 Torr of Ar in the previous papers[12,16] and has little dependence on v. The bimolecular rate coefficients, $k_v^{\mathrm{CF_4}}$, for vibrational relaxation of $O_2(X^3\Sigma_g^-, v = 6-12)$ by CF_4 have been determined and are listed in Table 1 along with the previously reported rate coefficients for other relaxation partners.

There are four vibrational modes in CF_4: ν_1(909 cm^{-1}), ν_2(435 cm^{-1}), ν_3(1281 cm^{-1}), and ν_4(632 cm^{-1});[36,37] ν_1 is nondegenerate (a_1), ν_2 is doubly degenerate (e), and ν_3 and ν_4 are triply degenerate (f_2). The latter two modes are infrared-active. The vibrational quantum energies of $O_2(X^3\Sigma_g^-)$, $\Delta G_{v+1/2}$, ranging from 1441 cm^{-1} for $v = 5$ to 1304 cm^{-1} for $v = 11$. The energy mismatch $|\Delta E|$ in the following process

$$\mathrm{O_2}\left(\mathrm{X}^3\Sigma_g^-, v\right) + \mathrm{CF_4}(v_i = 0) \rightarrow \mathrm{O_2}\left(\mathrm{X}^3\Sigma_g^-, v - 1\right) + \mathrm{CF_4}(v_i = 1) + \Delta E \quad (17)$$

for ν_3 mode ($i = 3$) is relatively small and decreases from 160 ($v = 6$) to 23 cm^{-1} ($v = 12$), and the other three vibrations have large energy mismatches for $v = 6-12$: $|\Delta E| > 395$ cm^{-1} for ν_1, > 869 cm^{-1} for ν_2, and > 672 cm^{-1} for ν_4. Of the fundamental vibrational modes, the ν_3 vibration is the most probable energy-accepting mode. However, it should be noted that the overtone and combination levels, $2\nu_4$(1264 cm^{-1}), $\nu_1 + \nu_2$(1344 cm^{-1}), $\nu_1 + \nu_4$(1541 cm^{-1}), and $\nu_2 + \nu_4$(1067 cm^{-1}), might be effective at energy transfer with $O_2(X^3\Sigma_g^-, v = 6-12)$ because the $|\Delta E|$ of the $2\nu_4$ and $\nu_1 + \nu_2$ vibrations is as small as those of the ν_3 fundamental vibration. Although each of these vibrations may make a relatively small contribution to the relaxation, there might be nonnegligible effects in sum total.

The rate coefficients for V−T and V−V energy transfer by the same collision partners are generally in proportion to the vibrational quantum number v on the assumption of the harmonic oscillator,[38,39] and it is usual to divide the rate coefficients by v to isolate the effect of the energy mismatch $|\Delta E|$. Figure 4a shows the vibrational level dependence of $k_v^{\mathrm{CF_4}}/v$ obtained in the present study on the energy transfer between $O_2(X^3\Sigma_g^-, v = 6-12)$ by collisions with CF_4. Although we see seemingly good linear correlation between the rate coefficients of energy transfer and energy mismatch, generally accepted scaling laws of the energy-transfer process are exponential gap and power gap laws.[40]

An important factor governing energy-transfer processes is the adiabaticity parameter, ξ,[41−43] defined by

$$\xi = \frac{a|\Delta E|}{h\mathrm{v}} \quad (18)$$

where a is the range of the intermolecular force, $|\Delta E|$ is the energy mismatch (energy difference between before and after the events), v is a relative velocity during the collision,[44] and h is Planck's constant. There is a general rule that the efficiency of energy transfer with $\xi < 1$ (diabatic or high-velocity regime) is higher than that with $\xi > 1$ (adiabatic or low-velocity regime) and that the exponential energy gap law, $k \propto \exp(-\xi)$ is satisfied in the range of $\xi > 1$ (for example, ref 41 and Figure 5.9 therein). The energy mismatch corresponding to the transition condition $\xi = 1$ is estimated to be $|\Delta E| = 88$ cm^{-1} in the O_2-CF_4 case; v = 5.2 $\times$ 10^2 m s^{-1} at 298 K and an estimate $a \approx 0.2$ nm.[41−43] Figure 4b is a semilogarithmic plot $k_v^{\mathrm{CF_4}}/v$ versus $|\Delta E|$ and clearly shows the transition behavior of the efficiency of energy transfer between $O_2(v)$ and CF_4. The rate coefficients for low vibrational levels $v = 6-8$ in the adiabatic regime can be represented by the form of the exponential gap law, $b\mathrm{e}^{-c|\Delta E|}$. The level $v = 9$ is at the transition regime $\xi = 1.05$ with $|\Delta E| \approx 91$ cm^{-1}, and the levels $v \geq 10$ are in the diabatic regime. The linear correlation between $k_v^{\mathrm{CF_4}}/v$ and $|\Delta E|$ shown in Figure 4a might, therefore, be an accidental result over the adiabatic and diabatic regimes.

Figure 5 shows the rate coefficients for vibrational energy transfer from $O_2(X^3\Sigma_g^-)$ to several collision partners (the values are listed in Table 1). On the basis of the magnitudes of the energy mismatch and infrared activity, the most probable energy-accepting

vibrational modes are ν_1(1333 cm^{-1}) of CO_2, ν_1(1318 cm^{-1}) of NO_2, ν_3(1285 cm^{-1}) of N_2O, ν_4(1306 cm^{-1}) of CH_4, and ν_3(1281 cm^{-1}) of CF_4. Although the ν_1 vibration of CO_2 is infrared-inactive, infrared-active ν_2(667 cm^{-1}) and ν_3(2249 cm^{-1}) have too large energy mismatches. As seen in Figure 5, CF_4 is a dominantly efficient relaxation partner of O_2. The efficiencies of energy transfer are sensitive to the energy mismatches, and comparison must be made for vibrational levels with $|\Delta E|$ close in value. For example, $|\Delta E|$ between $O_2(v = 8)$ and CO_2, $v = 9$ and NO_2, $v = 10$ and N_2O, $v = 9$ and CH_4, and $v = 10$ and CF_4 is 62, 54, 65, 66, and 69 cm^{-1}, respectively, and the efficiency goes in the order $k_8^{CO_2} < k_9^{NO_2} < k_{10}^{N_2O} < k_9^{CH_4} \ll k_{10}^{CF_4}$. The fundamental infrared intensity A of the vibrational mode of the relaxation partners in units of the HITRAN[45] database is defined by the following equation:

$$A = \frac{1}{cl}\int \log_e \frac{I_0}{I} d\nu \qquad (19)$$

where c is the number density of the gaseous sample, l is a path length, ν is the wavenumber, and I_0 and I are the intensities of incident and transmitted light. The integral interval is over the single vibrational band of interest. The infrared intensities are ~0.4, ~70, ~30, ~1000 km mol^{-1} for $NO_2(\nu_1)$,[46] $N_2O(\nu_3)$,[47] $CH_4(\nu_4)$,[48] and $CF_4(\nu_3)$,[49]respectively, showing a relatively good correlation with the rate coefficients for energy transfer with $O_2(v)$.

Summary

Kinetic study on the relaxation of a wide range of vibrational levels $v = 6-12$ of $O_2(X^3\Sigma_g^-)$ by collisions with CF_4 has been performed based on the originally developed integrated profiles method (IPM). CF_4 is the most efficient relaxation partner in polyatomic molecules (CO_2, NO_2, N_2O, and CH_4) studied so far. The relatively small energy mismatches, 23 $cm^{-1} < |\Delta E| < 160$ cm^{-1} between $O_2(v = 6-12)$ and the triply degenerate C−F stretching vibration (ν_3) of CF_4 mainly governs the fast V−V energy transfer. The apparent failure in the exponential gap law has been accounted for by the transition behavior of $\xi > 1$ for $v \leq 8$ and $\xi < 1$ for $v \geq 10$. The extraordinarily large efficiency of CF_4 is elucidated by the very large fundamental infrared intensity (~1000 km mol^{-1}) of the ν_3 vibration.

Acknowledgment. The authors gratefully acknowledge Professor Hironobu Umemoto for equipment provision. This work was supported by a Grant-in-Aid for Exploratory Research (Contract No. 15655005) and a Grant-in-Aid for Scientific Research (B) (Contract No. 18350011) of the Japanese Ministry of Education, Culture, Sports, Science, and Technology. Support also was provided by Matsuo Foundation.

References and Notes

(1) Hocker, L. O.; Kovacs, M. A.; Rhodes, C. K.; Flynn, G. W.; Javan, A. *Phys. Rev. Lett.* **1966**, *17*, 233.
(2) Yardley, J. T.; Moore, C. B. *J. Chem. Phys.* **1966**, *45*, 1006.
(3) Yardley, J. T.; Moore, C. B. *J. Chem. Phys.* **1968**, *49*, 1111.
(4) Moore, C. B.; Wood, R. E.; Hu, B. B.; Yardley, J. T. *J. Chem. Phys.* **1967**, *46*, 4222.
(5) Silva, M.; Jongma, R.; Field, R. W.; Wodtke, A. M. *Annu. Rev. Phys. Chem.* **2001**, *52*, 811.
(6) Mack, J. A.; Mikulecky, K.; Wodtke, A. M. *J. Chem. Phys.* **1996**, *105*, 4105.
(7) Park, H.; Slanger, T. G. *J. Chem. Phys.* **1994**, *100*, 287.
(8) Klatt, M.; Smith, I. W. M.; Tuckett, R. P.; Ward, G. N. *Chem. Phys. Lett.* **1994**, *224*, 253.
(9) Klatt, M.; Smith, I. W. M.; Symonds, A. C.; Tuckett, R. P.; Ward, G. N. *J. Chem. Soc., Faraday Trans.* **1996**, *92*, 193.
(10) Hickson, K. M.; Sharkey, P.; Smith, I. W. M.; Symonds, A. C.; Tuckett, R. P.; Ward, G. N. *J. Chem. Soc., Faraday Trans.* **1998**, *94*, 533.
(11) Hernández, R.; Toumi, R.; Clary, D. C. *J. Chem. Phys.* **1995**, *102*, 9544.
(12) Yamasaki, K.; Fujii, H.; Watanabe, S.; Hatano, T.; Tokue, I. *Phys. Chem. Chem. Phys.* **2006**, *8*, 1936.
(13) Yamasaki, K.; Watanabe, A. *Bull. Chem. Soc. Jpn.* **1997**, *70*, 89.
(14) Yamasaki, K.; Watanabe, A.; Kakuda, T.; Tokue, I. *Int. J. Chem. Kinet.* **1998**, *30*, 47.
(15) Yamasaki, K.; Taketani, F.; Tomita, S.; Sugiura, K.; Tokue, I. *J. Phys. Chem. A* **2003**, *107*, 2442.
(16) Watanabe, S.; Usuda, S.-y.; Fujii, H.; Hatano, H.; Tokue, I.; Yamasaki, K. *Phys. Chem. Chem. Phys.* **2007**, *9*, 4407.
(17) Warneck, P. *Chemistry of the Natural Atmosphere*, 2nd ed.; Academic Press: London, 2000.
(18) Atkinson, R.; Baulch, D. L.; Cox, R. A.; Crowley, J.; Hampson, R. F., Jr.; Kerr, J. A.; Rossi, M. J.; Troe, J. IUPAC Subcommittee on Gas Kinetic Data Evaluation, Data Sheet POx2, 2001; http://www.iupac-kinetic.ch.cam.ac.uk/.
(19) Sander, S. P.; Friedl, R. R.; Golden, D. M.; Kurylo, M. J.; Huie, R. E.; Orkin, V. L.; Moortgat, G. K.; Ravishankara, A. R.; Kolb, C. E.; Molina, M. J.; Finlayson-Pitts, B. J. *Chemical Kinetics and Photochemical Data for Use in Atmospheric Studies, Evaluation No. 14*; Jet Propulsion Laboratory, California Institute of Technology: Pasadena, CA, 2003.
(20) Baiamonte, V. D.; Hartshorn, L. G.; Bair, E. J. *J. Chem. Phys.* **1971**, *55*, 3617.
(21) Webster, H., III; Bair, E. J. *J. Chem. Phys.* **1972**, *57*, 3802.
(22) Rogaski, C. A.; Mack, J. A.; Wodtke, A. M. *Faraday Discuss.* **1995**, *100*, 229.
(23) Jongma, R. T.; Wodtke, A. M. *J. Chem. Phys.* **1999**, *111*, 10957.
(24) Blitz, M. A.; Dillon, T. J.; Heard, D. E.; Pilling, M. J.; Trought, I. D. *Phys. Chem. Chem. Phys.* **2004**, *6*, 2162.
(25) Takahashi, K.; Kishigami, M.; Taniguchi, N.; Matsumi, Y.; Kawasaki, M. *J. Chem. Phys.* **1997**, *106*, 6390.
(26) Chiu, S. S.-L.; Cheung, A. S.-C.; Finch, M.; Jamieson, M. J.; Yoshino, K.; Dalgarno, A.; Parkinson, W. H. *J. Chem. Phys.* **1992**, *97*, 1787.
(27) Cosby, P. C.; Park, H.; Copeland, R. A.; Slanger, T. G. *J. Chem. Phys.* **1993**, *98*, 5117.
(28) Julienne, P. S.; Krauss, M. *J. Mol. Spectrosc.* **1975**, *56*, 270.
(29) Julienne, P. S. *J. Mol. Spectrosc.* **1976**, *63*, 60.
(30) Slanger, T. G.; Copeland, R. A. In *Advanced in Chemical Kinetics*; Barker, J. R., Ed.; JAI Press: Greenwich, CT, 1994; Vol. 2.
(31) Herzberg, G. *Molecular Spectra and Molecular Structure, I. Spectra od Diatomic Molecules*; Van Nostrand Reinhold: New York, 1950.
(32) Harris, R.; Blackledge, M.; Generosa, J. *J. Mol. Spectrosc.* **1969**, *30*, 506.
(33) Geiser, J. D.; Dylewski, S. M.; Mueller, J. A.; Wilson, R. J.; Toumi, R.; Houston, P. L. *J. Chem. Phys.* **2000**, *112*, 1279.
(34) Yamasaki, K.; Taketani, F.; Sugiura, K.; Tokue, I. *J. Phys. Chem. A* **2004**, *108*, 2382.
(35) Demas, J. N. *Excited State Lifetime Measurements*; Academic Press: New York, 1983.
(36) Shimanouchi, T. *Tables of Molecular Vibrational Frequencies Consolidated Volume I*; National Bureau of Standards: Washington, DC, 1972; pp 1−160.
(37) Stein, S. E. Infrared Spectra. In *NIST Chemistry WebBook, NIST Standard Reference Database Number 69*; Lindstrom, P. J., Mallard, W. G., Eds.; National Institute of Standards and Technology: Gaithersburg, MD, 2005; http://webbook.nist.gov.
(38) Hancock, G.; Smith, I. W. M. *Appl. Opt.* **1971**, *10*, 1827.
(39) Yardley, J. T. *Introduction to Molecular Energy Transfer*; Academic Press: New York, 1980.
(40) Houston, P. L. *Chemical Kinetics and Reaction Dynamics*; McGraw-Hill: Boston, MA, 2001.
(41) Levine, R. D.; Bernstein, R. B. *Molecular Reaction Dynamics*; Oxford University Press: New York, 1974.
(42) Levine, R. D.; Bernstein, R. B. *Molecular Reaction Dynamics and Chemical Reactivity*; Oxford University Press: New York, 1987.
(43) Levine, R. D. *Molecular Reaction Dynamics*; Cambridge University Press: Cambridge, U.K., 2005.
(44) Velocity is denoted by Roman v, vibrational quantum number by italic v, and frequency by Greek ν throughout this article.
(45) Rothman, L. S.; Barbe, A.; Chris Benner, D.; Brown, L. R.; C.-Peyret, C.; Carleer, M. R.; Chance, K.; Clerbaux, C.; Dana, V.; Devi, V. M.; Fayt, A.; Flaud, J.-M.; Gamache, R. R.; Goldman, A.; Jacquemart, D.; Jucks, K. W.; Lafferty, W. J.; Mandin, J.-Y.; Massie, S. T.; Nemtchinov, V.; Newnham, D. A.; Perrin, A.; Rinsland, C. P.; Schroeder, J.; Smith, K. M.; Smith, M. A. H.; Tang, K.; Toth, R. A.; Auwera, J. V.; Varanasi, P.; Yoshino, K. *J. Quant. Spectrosc. Radiat. Trans.* **2002**, *82*, 5.
(46) Perrin, A.; Flaud, J.-M.; Camy-Peyret, C.; Vasserot, A.-M.; Guelachvili, G.; Goldman, A.; Murcray, F. J.; Blatherwick, R. D. *J. Mol. Spectrosc.* **1992**, *154*, 391.
(47) Łapiński, A.; Spanget-Larsen, J.; Waluk, J.; Radziszewski, J. G. *J. Chem. Phys.* **2001**, *115*, 1757.
(48) Galabov, B.; Yamaguchi, Y.; Remington, R. B.; Schaefer, H. F., III *J. Phys. Chem. A* **2002**, *106*, 819.
(49) de Oliveira, A. E.; Haiduke, R. L. A.; Bruns, R. E. *Spectrochim. Acta, Part A* **2000**, *56*, 1329.

JP802201M